NUMERICAL SIMULATION OF FLAPPING WING AERODYNAMIC PERFORMANCE UNDER GUST WIND CONDITIONS

Tung Wan, Chian-kuei Huang
Department of Aerospace Engineering, Tamkang Univeristy
Tamsui, Taiwan, ROC

Keywords: *Flapping wing, Dynamic mesh, Severe weather conditions*

Abstract

Studies about flapping wing aerodynamic performance have been only concentrated on motion under calm and clear atmospheric conditions. Small atmospheric disturbance such as gust wind could lead to flapping MAV (Micro Aerial Vehicle) great damage. In this study, using numerical method and employ FLUENT software as the flow solver, the motions of flapping wing are simplified and combined with the dynamic mesh technique. Thus we could calculate the 2-D flapping wing aerodynamic parameters such as lift and thrust in unsteady flow. Finally, the flapping wing behavior is simulated in gust wind conditions through existing gust wind profile, and results show that the lift did change with the wind speed. As wind speed becomes larger, the lift also varies violently and may lead to detrimental situations. Weather influence always exists, and must be included in MAV design consideration, thus current study represent a preliminary investigation in that aspect.

1 Introduction

While aeronautical technology has advanced rapidly over the past 100 years, nature's flying animals have already evolved over 150 million years and still going on. Generally, flight can be separated into two different forms– bird flight and insect flight. Although these two kinds of flight are based on flapping motion, there are discrepancies between them. Most birds flap their wing in vertical stroke plane with small change in angle of attack of their wing while flying. However, insects fly by their flapping wings that generate a lot of vortices. Especially in hovering, they need a sea of vortices to keep them aloft. Therefore, to understand how insects fly, we have to picture how the vortices shed from flapping wings. Because flapping wings have the characteristics of small size, low Reynolds number, and rapidly, complex flapping mechanism, there is no simple theory to explain how insects fly. At low Reynolds number, flow around flapping wings behave in an unsteady fashion, usually accompanied by complex vortex break-down, separation, and reattachment, quite different from those well-known flow behaviors at high Reynolds numbers.

Flapping wing propulsion has recently gained attraction by the rising interest in alternative propulsion systems for MAVs (Micro Aerial Vehicles), which have smaller size and lower speed relative to UAV (Unmanned Aerial Vehicle). A number of small aircraft with flapping wings, known as ornithopters, have already made the first flight. As Shyy et al. [1] have pointed out that the specification for MAVs restricts the flight regime of such vehicles to low Reynolds number by enforcing similarity to birds with respect to cruising speed. Flapping wings are therefore assumed to be an appropriate means to efficiently propel such vehicles.

It also has been shown that conventional aerodynamic theory, which was based on steady flow condition, cannot explain the generation of lift by flapping insects. In the past year of studies, scientists have found that unsteady flow condition can't be neglected in flapping motion. Early "quasi-steady assumption" tried to predict the unsteady and highly efficient flapping motion, hence leads to the myth "bumblebees cannot fly". The essence of quasi-steady analysis is an assumption that the instantaneous force on a flapping wing to be the same as that which would be experienced in steady motion at the same instantaneous velocity and angle of attack [3]. Such assumption is obviously unrealistic and lack of accuracy. Thus, a better representation of flapping wing motion is urgently needed.

Insect-like MAV is very small and light, and is easily influenced by atmospheric disturbances. Therefore, how to fly in unstable weather will be a difficult problem to design an insect-like MAV in future. According the definition of DARPA (Defense Advanced Research Project Agency), MAV with spans of 15cm or less and flight speed under 10m/s are of interest of military and civilian application. In recent years, there are renewed interests in the usage of insect-like MAV, especially for military, surveillance, and rescue missions [3]. But it is expected that all insect-like MAVs should perform the mission in the calm and clear atmospheric conditions, i.e. no gust wind exists. For some time, our research group has investigated fixed-wing aircraft performance degradation effects under many severe weather conditions such as microburst, clear air turbulence, ice accretion, and heavy rain. Now the attention has shifted to flapping wing numerical study with severe weather conditions. For fixed wing machines, weather always plays an important role, especially in take-off and landing. However, flapping wing machines are much small than fixed wing machines, thus the weather influence will be much more important and becomes the focus of this research.

In this study, CFD (Computational Fluid Dynamics) technique will be used to investigate the flapping wing aerodynamic efficiency under gust wind. Base on previous literatures, this study is the first to combine the numerical gust wind model and flapping wing mechanism. While the research on the topic is still at a beginning stage, the findings on this study may have broad implications in future MAV design.

2 Literature Review

Early, researchers used "quasi-steady" assumption to the lift produced by flapping flyers but they found the lift couldn't keep the insect aloft. In 1973, Weis-Fogh first found the unconventional lift that called "clap and fling" [4]. He proposed that air rushing into the space created, as the separated wings would form attached circulations that create large amount of lift, but it is limited to a few species of insects. Another famous unsteady lift enhancement mechanism is delayed stall due to the leading edge vortex (LEV). When insect wing translates at high angles of attack, a vortex forms on the leading edge of a wing that can generate forces in excess of those predicted under quasi-steady state conditions.

In the mid 1980s, C.P. Ellington [3, 5] observed the LEV by smoking visualization and started to investigate the different aspects of hovering insect flight. By using high-speed camera, he observed flying insects and tried to use reverse engineering to figure out the mechanism of flapping wing. Gustafson and Leben [6,7] used a 2D Navier-Stokes solver to compute the unsteady flows around an airfoil undergoing plunging and pitching motions and obtained results very similar to those of a 2D wing model experiment by Freymuth [8]. Calculations of the 3D flow around flapping wings are also available with respect to time-dependent forces, but results for mean thrust output and efficiency are rarely found.

In 1996, Vest and Katz [9] developed a potential flow, unsteady aerodynamic model of flapping wings and gives a good estimation of the pressure forces on the body and determines the valuable aerodynamic parameters like lift and drag. Navier-Stokes solutions for the viscous flow around 2D wings have been presented by Wang [10] and found that the lift that produced by flapping wing can keep the insect aloft. Miao at el. [11] found that the thin airfoil could produce more lift and more efficiency. Liu and Kawachi [12] demonstrated the existence and stability of the unsteady leading edge vortex on a simulation of the hawkmoth wing.

Recently, because CFD (Computational Fluid Dynamics) came to maturity, there are more and more researches using CFD technique to analyze flapping wing phenomenon. Sun, et al. used CFD code studying how could insects aloft in hovering, and interaction between wings [13].

In nature, birds and bats will twist and bend their wing for optimal lift and thrust while maneuvering. Ho at el. found that wing flexibility is important for flapping wing [14]. Smith [15] commented on the importance of flexibility and wing stiffness in accurately modeling the flapping motion and the resultant force generation. Shyy et al. [16] conducted a systematic numerical study of adaptive airfoils in response to oscillatory flows and found that passive airfoils that deform in accordance with the local pressure distribution can increase the lift coefficient significantly.

According to the author's best knowledge, although there are numerous research works on flapping wing aerodynamic performance, but none of them seem to consider the degradation effects on severe weathers. Thus it is believed that this study represents a major forward step in flapping wing aerodynamic computation.

3 Numerical Method

In real world, the flapping motion is 3-D mechanism, unsteady with complex flow patterns. As a first step, we currently only consider 2-D behavior. Before building numerical model, we have to take following assumptions: (1) the wing section is elliptic and the thickness is 1/8 of chord length (2) the flapping motion is along stroke plane, (3) laminar and unsteady flow (4) wing is a rigid body.

Fig. 1 shows the position of wing motion in one period. In real case, the motion of flapping wing is in figure 8 shapes. In this study, the flapping motion of a wing is simplified to 2 equations as follows. The wing translates downward and upward along the stroke plane that inclines an angle β and rotates during stroke reverses. The displacement of flapping wing is denoted by $A(t)$ and is given by:

$$A(t) = \frac{A_0}{2}[\cos(2\pi\omega t + \gamma) + 1] \qquad (1)$$

where A_0 is amplitude; ω is stroke frequency ; t is time, and γ is the phase angle of the translation of the wing and the stroke plane is inclined at an angle β. Angle of attack of flapping motion is denoted by $\alpha(t)$ and is given by:

$$\alpha(t) = \frac{\pi}{4} - \frac{\pi}{4}\sin(2\pi\omega t + \gamma) \qquad (2)$$

In analysis of flying motion, the most important physical parameters are: characteristic length of flapping wing (L), flapping frequency (ω), flying velocity (U), fluid viscosity (μ), and fluid density (ρ). In this study, we consider the fluid is incompressible, so that we can combine the viscosity and density into kinematic viscosity (ν_k). There are two dimensionless parameters can be derived from L, ω, U and ν_k: Reynolds number ($\mathrm{Re} = UL/\nu_k$) and Strouhal number ($St = \omega L/U$). Reynolds number represents the ratio of inertial force and viscous force. When Re is small, the viscous force is more important. Strouhal number presented the characteristic of flapping and flying speed. If we choose the chord length (c) as characteristic length, the Strouhal number becomes to be reduced frequency ($k_r = \omega c/U$).

The software that used in this study is FLUENT, which solves Navier-Stokes equations in finite volume method. The grids we used combined with quadrilateral and triangular grids as Fig. 2. The flapping motion contains a series of translation and rotation, so the flow field is also complex. To predict the flow pattern accurately, construct a suitable mesh system is necessary and the dynamics mesh also has to be considered. The region near the flapping wing will be constructed as O-type structure grids because there are more variations of pressure and velocity. O-type structure grids can maintain highly orthogonal during mesh motion. In the region between rectangular and triangle cell, we found that the volume between these two cells must be similar to each other. The advantage of using hybrid grids is when the grids move in every time step, only the outer triangle grids will regenerate and the rectangular grids around the flapping wing will move with flapping motion synchornously.

For all flows, FLUENT solves consevation equations of mass and momentum. The equaitons for conservation of mass and momentum can be combined as following equation in dyanamic mesh form:

$$\frac{d}{dt}\int_V \rho\phi dV + \int_{\partial V} \rho\phi(\vec{v} - \vec{v}_g)\cdot d\vec{A} = \int_{\partial V} \Gamma\nabla\phi\cdot d\vec{A} + \int_V S_\phi dV \quad (3)$$

where ρ is the fluid density

$\vec{v}$ is the flow velocity vector

$\vec{v}_g$ is the grid velocity of the moving mesh

Γ is the diffusion coefficient

S_ϕ is the source term of ϕ

ϕ is the user scalar

In this study, to simulate the real surrounding environment, we set the pressure boundary condition and set to be zero initially. During calculation, we use the second order implicit discretization in time, and in momentum, we could use the QUICK scheme. Finally, the PISO algorithm is implemented to discrete the velocity-pressure coupling term. Although the implicit method takes more computing time but it is much stable in every time step.

Secondly, we constructed the gust wind model to simulate the real case that MAVs could face in their flight. Although the Von Karman model and The Dryden PSD (Power Spectrum Density) model are used to simulate the atmospheric turbulence widely, they are somewhat difficult to use in time domain. In this study, we use different approach to simulate 2-D gust wind profiles. The model is given in terms of atmospheric turbulence velocity components that can be considered as fluctuations superposed on a mean wind. As a first step, the existing high level turbulence wind profiles could assumed as strong low level gust wind. Before we proceed with building gust wind model, we must define turbulence intensity first. We use the high altitude CAT (Clear Air Turbulence) prediction parameters to quantify the wind severity (T_1) [20] and verify the turbulence intensity between the real wind and the wind we created. T_1 factor can be defined as:

$$T_1 = \sum_{i=1}^{3} \left| \frac{\dot{W}_i}{g} \right| \quad (4)$$

where $\dot{W}_i$ is turbulence wind acceleration in 3 different directions and g is gravitational constant. Thus T_1 represents the severity of 3-D wind. Fig. 3 and Fig.4 show the turbulence model has large fluctuation in both X and Y direction. These two gust wind models are basis on high altitude phenomena. In nature, insects usually fly at low level altitude (less than 500m) and hardly suffer gust wind similar to the model we built. Although ordinary flapping flight insects hardly ever encounter these wind profiles, but still it could represent the most severe weather conditions that an insect might face, so still being considered here.

4 Verification

In order to validate the accuracy of computational results, a benchmark case is necessary to consider. First, we considered an example, which the approximation of Navier-Stokes equation is known. Secondly, we compare the computed result with theoretical one. Finally, we compare the unsteady flow field computed from FLUENT with well-documented experiment by Bouard and Coutanceau [21] in 1980 and different numerical solution computed from Wang [22].

Considering impulsively started flow over a cylinder, due to the no-slip boundary condition, a thin boundary layer builds up. The flow outside the boundary layer can be described by the potential flow:

$$\Psi = -U_0\left(r - \frac{R^2}{r}\right)\sin\theta \quad (5)$$

$$u_r(r) = U_0\left(1 - \frac{R^2}{r^2}\right)\cos\theta \quad (6)$$

$$u_\theta(r) = -U_0\left(1 + \frac{R^2}{r^2}\right)\sin\theta \quad (7)$$

where U_0 is the velocity of the cylinder and R is the radius.

We construct the grid system as Fig. 5, there are 11192 triangular cells and 16274 quadrilateral cells surrounding the cylinder with diameter 0.2m under Re=550.

In Fig. 6, we compute the velocity $u_\theta(r)$ and compare the result with the analytical solution as a function of r/R with fixed value of $\theta = \pi/2$ under Re=100. The numerical result agrees well with the potential solution outside the boundary layer.

Fig. 7 shows the result that computed in this study compares with the experiment by Bouard and Coutanceau and numerical simulation from Wang. The data is computed from the velocity field in the wake along the symmetry axis. Above verification shows that the result computed from FLUENT agrees well with the experiment and other numerical result. This gives us confidence to use similar numerical technique in computing more complicated problem.

5 Results and Discussion

Considering the flapping wing with thickness 1/8*c* and Re=157. In the study, the cases we calculated are in 3 conditions with different wind profiles and another case with no wind. First, we discuss the case without wind at Re=157. The sources of force are from pressure difference, viscous term is not too important in such case. During downstroke, we observed there are two rotating vortices on upper surface, which create a lower pressure area, and pressure difference generated which lead to lift. Before the vortices get rid of the wing surface, the delayed stall that discussed in Dickinson's experiment [21] occurs because the lower pressure on upper wing surface (Fig. 8). During upstroke, the wing also create a weaker vortices on lower surface, that lead to the wing generate thrust (Fig. 9). From Fig. 9, we can observe that the wing is sufficiently far away from the strong vortices generated in the previous cycle and is ready to repeat the whole process without interfering with the previous vortices.

We can integrate pressure on the wing that created by vortices to get lift and drag in unsteady flow. Fig. 10 shows the lift which change with time. From the 1st period to 3th period, we observed that the lift is not stable because the flow starts from the rest and more unstable. After the fifth period, the lift becomes more stable. Fig. 11 shows that Drag occurs in down stroke, but in upstroke, because of vortices, more thrust occurs. Another aerodynamic parameter is mean lift. Table 1 shows the mean lift in different reference. For the first three periods is unstable, we choose the forth to thirteen period to take time integration and average. Fig. 12 shows lift we calculated comparing with Wang [10] and Miao's [11]. Our pattern is similar to Wang's result, but the magnitude is similar to Miao's result. Besides the difference of grids, numerical method is also different from Wang's calculation that was using finite difference method. Comparing with Miao's calculation, we also used the different boundary treatment. In pressure outlet boundary, Miao used rectangular but we used the circle one and far away the flapping wing. In our calculation, we found that if the region of mesh regeneration is too close pressure outlet boundary, the error could occur because the reversed flow from pressure outlet boundary.

Table 1 Mean lift in numerical simulation.

	Wang[10]	Miao [11]	Present study
Mean lift	2.8e-2 N/m	3.083e-2 N/m	3.134e-2 N/m

From 2-D lift numerical simulation, we can estimate the lift of 3-D flapping wing. Considering a rectangular flapping wing with chord length=1cm, wingspan=5cm, the flapping wing can produce lift about 1.57e-3 N in which we neglected the 3-D relieving effect. A dragonfly weights about 0.25 gram (2.45e-3N), with 4 wings which generate about 6.28e-3 N. the lift is sufficient to aloft the dragonfly, which consist with Wang [10] and Miao's [11] simulation analysis.

What we interest is flapping wing aerodynamics in gust wind. In Fig. 13 and Fig. 15, we observed that the lift did change with wind and performance is much better than the case without wind. Considering the wind in X and Y direction in Fig. 14, we found that wind in Y direction is blowing upward, which provides an upward force to flapping wing. Fig. 17 shows the mean lift variation, with wind speed increase or decrease, the mean lift also change with wind speed and the pattern is similar with the wind in Y direction. Consider the drag in Fig. 16 and Fig. 18; we also observed the same trend as lift profile. From Fig. 19 to Fig. 24 show the different case with different wind profile. In case 2, we choose the increasing wind speed and the wind in Y direction blows downward. It also shows that the lift changed with wind speed. We could observe that in this case, more down force is produced by wind in Y direction. Case 3 shows increasing wind speed and positive wind in X direction but negative in Y direction. In Fig. 25 to Fig. 30, we also observe the same phenomena as above 2 cases, which the lift and drag vary with gust wind and might lead to crash flight situation.

Summarizing the above 3 cases, we can conclude that the flapping wing is easily influenced by surrounding environment especially in gust wind. Even the gust wind only changed in small variation condition, it could lead to a huge calamity to insects. It also explained that why we rarely observed insect's activities in environment with gust wind situation. This study also leads to the conclusion that severe gust wind condition is important consideration in designing the flapping MAV and in the future with proper adjustment in flapping motion it should be able to operate under such severe condition.

6 Conclusions

In this study, we confirmed that surrounding atmospheric environment easily influences the flapping wing. Our study shows that the wind can easily influence the lift and drag of flapping wing, especially in negative direction wind. The result also shows that flapping wing could suffer a negative force and is very difficult to control thus could lead the flapping wing to crash under gust wind situation. Although the result we calculated has no reference data to verify, but at least we have understood both qualitatively and quantitatively the detrimental effect of gust wind to flapping wing.

In nature, we already know that insects and birds can twist their wing to have optimal aerodynamic wing shape and response the ever-changing surrounding environment. The current research effort merely is the preliminary analysis in flapping wing aerodynamic computation under severe gust wind conditions. In the future, both the 3-D shape and flexibility of wings also can be considered. Furthermore, the rain effects and the flow control will be the next focus of such topics in our flapping wing simulation

Acknowledgement

The support of this work by the National Science Council, ROC, under the contract NSC 95-2221-E-032-013 is gratefully acknowledged.

References

[1] Shyy, W., M. Berg and D. Ljungqvist, "Flapping and Flexible Wings for Biological and Micro Air Vehicles," *Progress in Aerospace Sciences,* Vol. 35, pp. 455-505, 1999.

[2] Mueller, J. Thomas and J. D. DeLaurier, "An Overview of Micro Air Vehicle Aerodynamics," *Fixed and Flapping Wing Aerodynamics for Micro Air Vehicle Applications*, Vol. 195, pp. 1-9, 2001.

[3] Ellington, C.P. "Unsteady Aerodynamics of Insect Flight," *Symposia of the Society for Experimental Biology*, Vol. 49, pp. 109-129, 1995.

[4] Sane, S.P., "The Aerodynamics of Insect Flight," *J. of Exp. Biology,* Vol. 206, pp.4191-4208, 2003.

[5] Ellington, C.P. "The Aerodynamics of Hovering Insect Flight: III. Kinematics," *Philosophical Transactions of the Royal Society of London,* B.305, pp.41-78, 1984.

[6] Gustafson, K. and R. Leben, "Computation of Dragonfly Aerodynamics," *Computational Phys. Communication*, Vol. 65, No. 121, pp. 121-132, 1991.

[7] Gustafson, K., Leben, R. and J. McArthur, "Lift and Thrust Generation by an Airfoil in Hover Modes," *CFD Journal*, Vol. 1, pp. 47-57, 1992.

[8] Freymuth, P. "Thrust Generation by an Airfoil in Hover Modes," *Experiments in Fluids*, Vol. 9, No.1-2, pp. 17-24, 1990.

[9] Vest, M. S. and J. Katz, "Unsteady Aerodynamic Model of Flapping Wings," *AIAA Journal*, Vol.34, pp. 1435-1440, 1996.

[10] Wang, Z. J., "Two Dimensional Mechanism for Insect Hovering," *Physical Review Letters*, Vol. 85, No.10, pp. 2216-2219, 2000.

[11] Miao, J. M., M. H. Ho and C. H. Tai, "Numerical Approach to the Aerodynamic Characteristics of Low Reynolds Number Flapping-Wing Motion," *Transactions of the Aeronautical and Astronautical Society of the Republic of China*, Vol. 37, No.2, pp. 135-146, 2005.

[12] Liu, H. and K. Kawachi, "A Numerical Study of Insect Flight," *J. of Comp. Physics*, Vol. 146, No.1 pp. 124-156, 1998.

[13] Sun, M. and S. L. Lan, "A Computational Study of the Aerodynamic Force and Power Requirement of Tiny Dragonfly," *J. of Exp. Biology,* Vol. 207, pp. 1889-1907, 2004.

[14] Ho, S., H. Nassef, N. Pornsinsirirak, Y. C. Tai and C. M. Ho, "Unsteady Aerodynamics and Flow Control for Flapping Wing Flyers," *Progress in Aerospace Sciences*, Vol. 39, pp. 635-681, 2003.

[15] Smith, M. J. C., "Simulating Moth Wing Aerodynamics: Towards the Development of Flapping Wing Technology," *AIAA Journal*, Vol. 34, No.7, pp. 1348-1355, 1996.
[16] Shyy, W., D. A. Jenkins and R. W. Smith, "Study of Adaptive Shape Airfoils at Low Reynolds Number in Oscillatory Flow," AIAA Journal, Vol. 35, pp. 1545-1548, 1997.
[17] Ellington, C.P and J. R. Usherwood, "Lift and Drag Characteristics of Rotary and Flapping Wings," *Fixed and Flapping Wing Aerodynamics for Micro Air Vehicle Applications*, Vol. 195, pp. 231-246, 2001.
[18] Tennekes, H. and J. L. Lumley, *A First Course in Turbulence*, MIT Press Design Department, 1973.
[19] FLUENT 6.2's User Guide.
[20] Wan, T. and H. F. Huang, "Clear Air Turbulence Strategy Analysis via Genetic Algorithm and Neural Network Method," *AIAA paper* 2002-0941, 2002.
[21] Bouard, R. and M. Coutanceau, "The Early Stage of Development of the Wake Behind an Impulsively Started Cylinder for 40<Re<10^4," *Journal of Fluid Mechanics*, Vol. 101, pp.583-607, 1980.
[22] Wang, Z. J., "Vortex Shedding and Frequency Selection in Flapping Flight," *Journal of Fluid Mechanics*, Vol. 410, pp. 323-341, 2000.
[23] Dickinson, M. H., F. O. Lehmann and S. P. Sane, "Wing Rotation and the Aerodynamic Basis of Insect Flight," *Science*, Vol. 284, pp. 1954-1960, 1996.

Copyright Statement

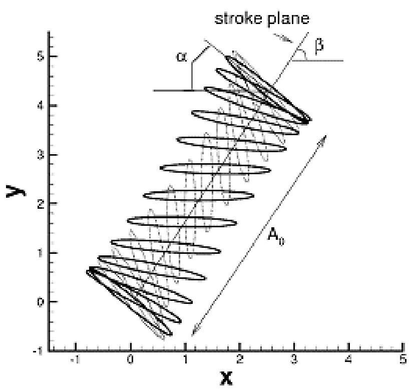

Fig.1 The positions of flapping wing in one period [10]

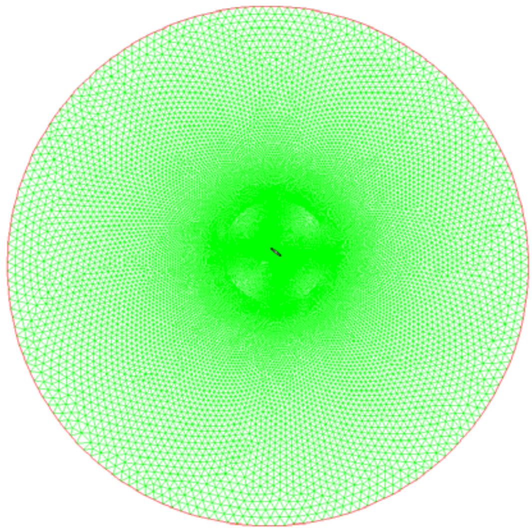

Fig.2 Grids and calculated field

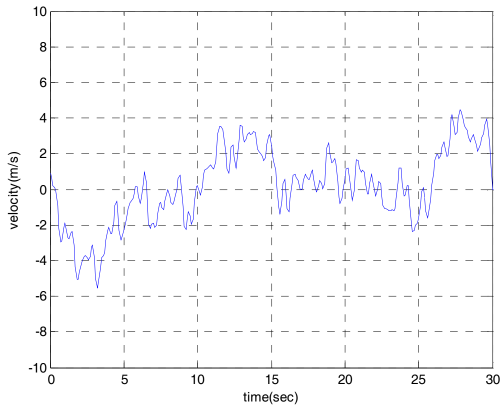

Fig. 3 X direction gust wind model velocity

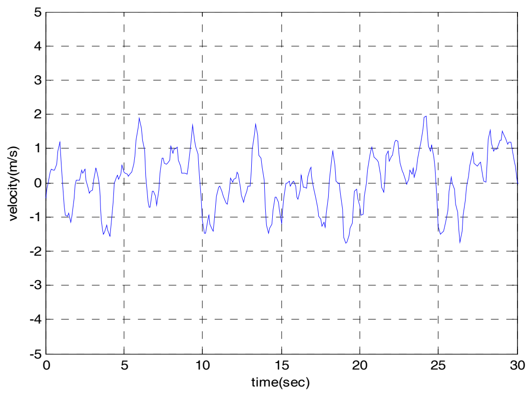

Fig. 4 Y direction gust wind model velocity

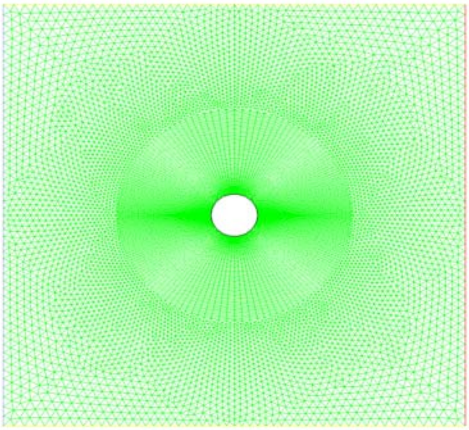

Fig. 5 The mesh in impulsively started flow over a cylinder

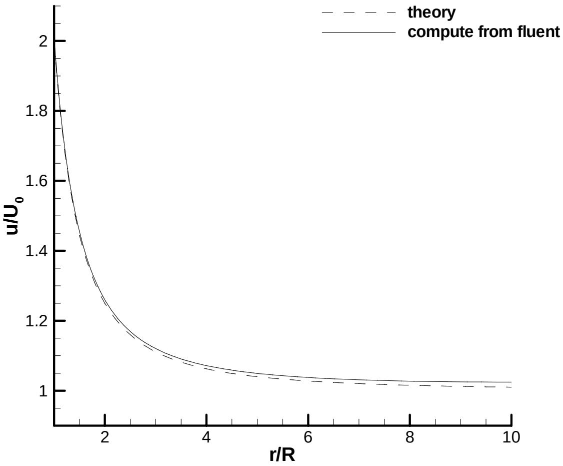

Fig. 6 Numerical result for velocity $u_\theta(r)$ vs. r/R compared with theory

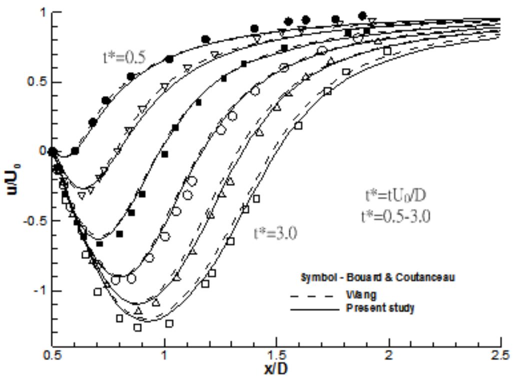

Fig. 7 The velocity along the symmetry axis at different instant

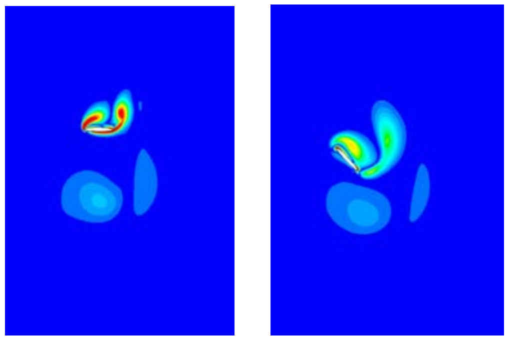

Fig. 8 Vorticity contour during downstroke

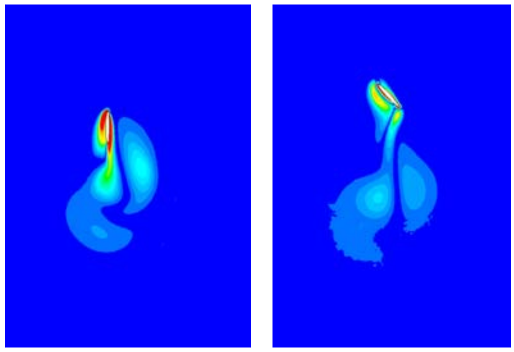

Fig. 9 Vorticity contour during upstroke

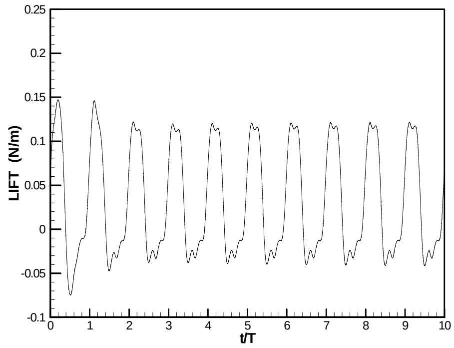

Fig. 10 Lift profile in first ten periods

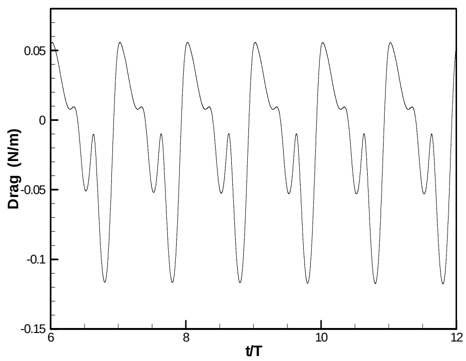

Fig. 11 Drag vs. period

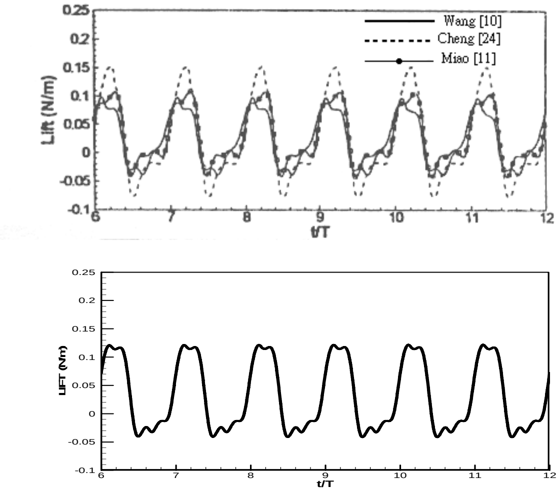

Fig. 12 Lift vs. period comparing with references

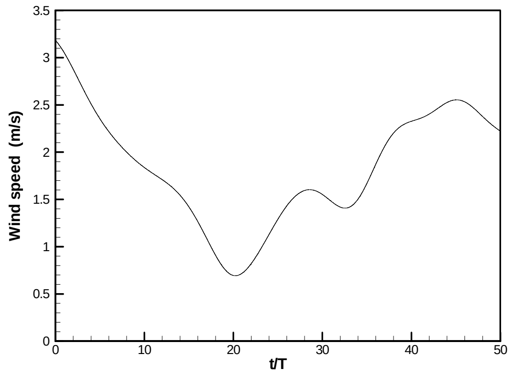

Fig. 13 Wind magnitude vs. period in case 1

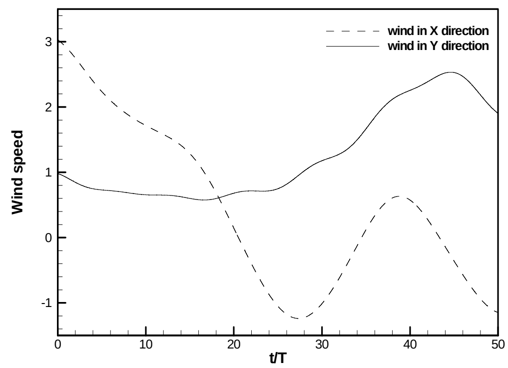

Fig. 14 Wind speed in different direction in case 1

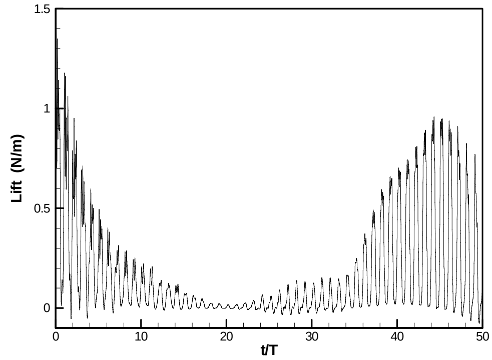

Fig. 15 Lift vs. period in case 1

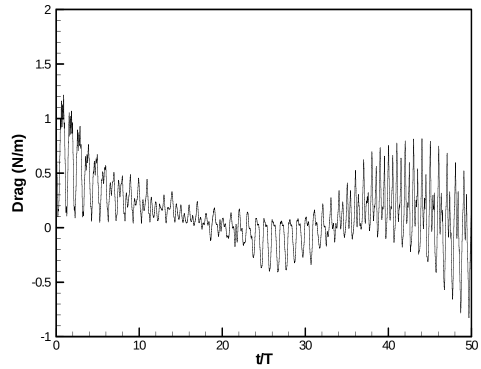

Fig. 16 Drag vs. period in case 1

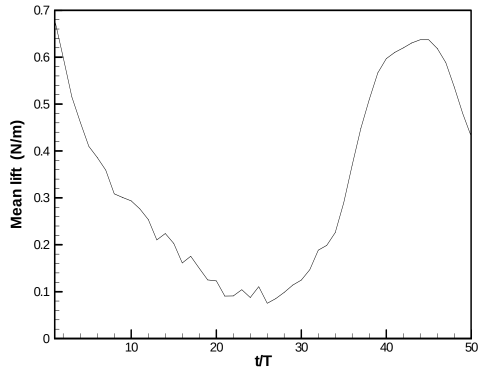

Fig. 17 Mean lift per period in case 1

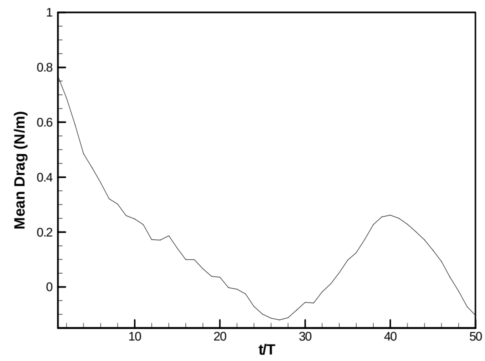

Fig. 18 Mean drag per period in case 1

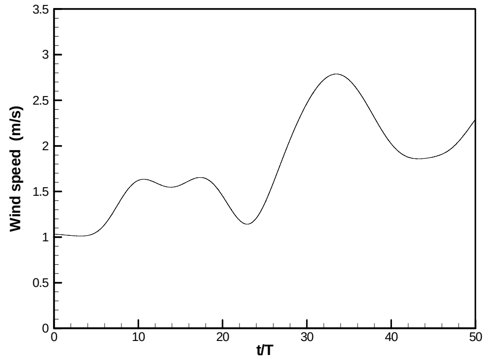

Fig. 19 Wind magnitude vs. period in case 2

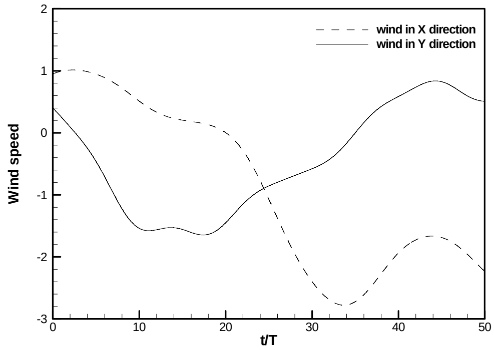

Fig. 20 Wind speed in different direction in case 2

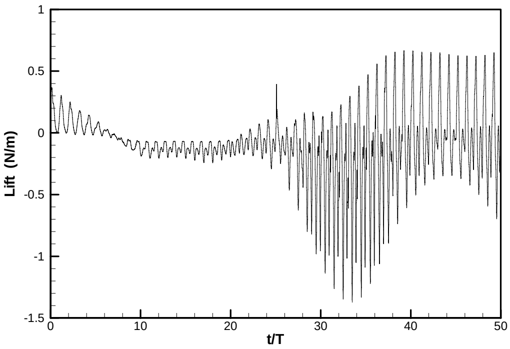

Fig. 21 Lift vs. period in case 2

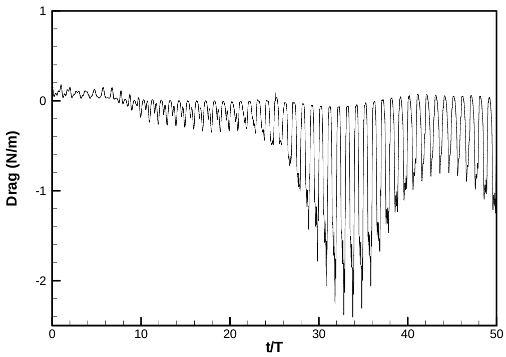

Fig. 22 Drag vs. period in case 2

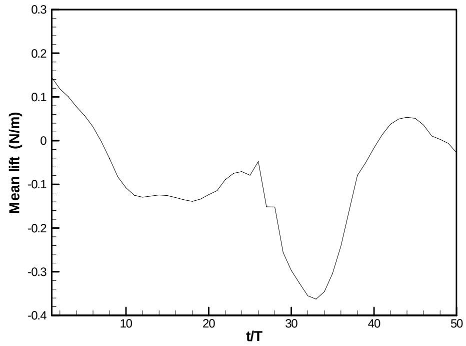

Fig. 23 Mean lift per period in case 2

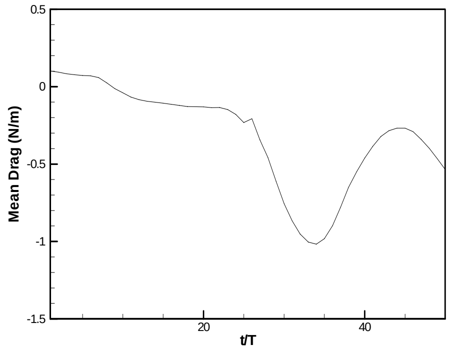

Fig. 24 Mean drag per period in case 2

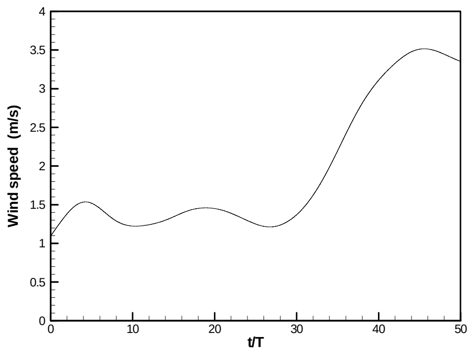

Fig. 25 Wind magnitude vs. period in case 3

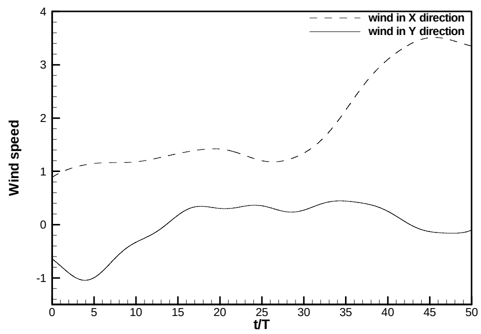

Fig. 26 Wind speed in different direction in case 3

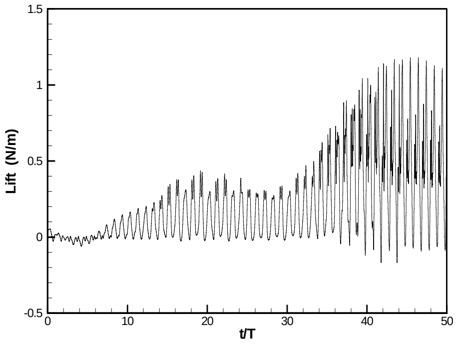

Fig. 27 Lift vs. period in case 3

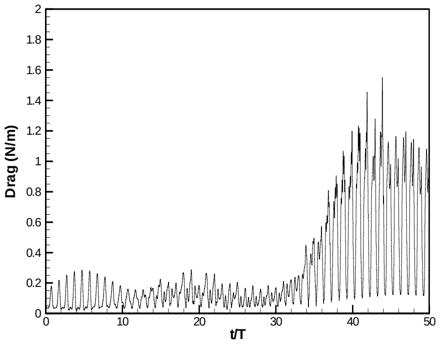

Fig. 28 Drag vs. period in case 3

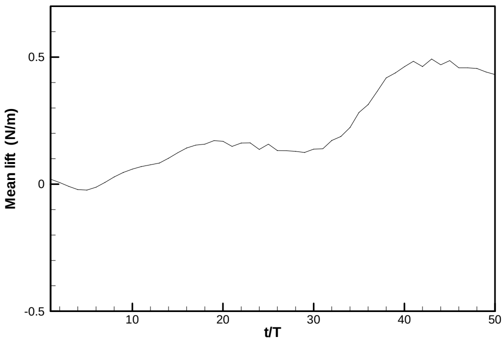

Fig. 29 Mean lift per period in case 3

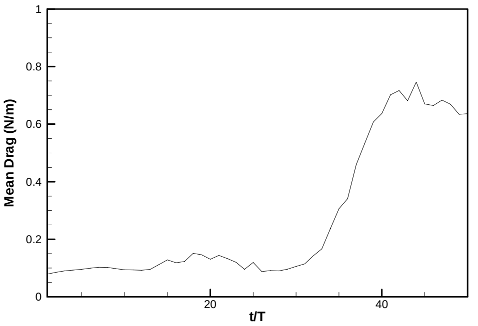

Fig. 30 Mean drag per period in case 3